arXiv:1605.05442v2 [cond-mat.dis-nn] 29 Jul 2016

Resilience of antagonistic networks with regard to the effects of initial failures and degree-degree correlations

Shunsuke Watanabe*
Department of Computational Intelligence and Systems Science, Tokyo Institute of Technology, Yokohama 2268502, Japan

Yoshiyuki Kabashima†
Department of Mathematical Intelligence and Systems Science, Tokyo Institute of Technology, Yokohama 2268502, Japan

(Dated: August 1, 2016)

In this study, we investigate the resilience of duplex networked layers (α and β) coupled with antagonistic interlinks, each layer of which inhibits its counterpart at the microscopic level, changing the following factors: whether the influence of the initial failures in α remains (quenched (Case Q)) or not (free (Case F)); the effect of intralayer degree-degree correlations in each layer and interlayer degree-degree correlations; and the type of the initial failures, such as random failures (RFs) or targeted attacks (TAs). We illustrate that the percolation processes repeat in both Cases Q and F, although only in Case F are nodes that initially failed reactivated. To analytically evaluate the resilience of each layer, we develop a methodology based on the cavity method for deriving the size of a giant component (GC). Strong hysteresis, which is ignored in the standard cavity analysis, is observed in the repetition of the percolation processes particularly in Case F. To handle this, we heuristically modify interlayer messages for macroscopic analysis, the utility of which is verified by numerical experiments. The percolation transition in each layer is continuous in both Cases Q and F. We also analyze the influences of degree-degree correlations on the robustness of layer α, in particular for the case of TAs. The analysis indicates that the critical fraction of initial failures that makes the GC size in layer α vanish depends only on its intralayer degree-degree correlations. Although our model is defined in a somewhat abstract manner, it may have relevance to ecological systems that are composed of endangered species (layer α) and invaders (layer β), the former of which are damaged by the latter whereas the latter are exterminated in the areas where the former are active.

I. INTRODUCTION

Our real world is composed of a huge variety of systems, which function in various layers, such as technology, society, and biology, and are continuously growing in unstable environments. It is thus of great importance to capture the essence of these complex critical systems. The *graph* [1, 2] or *network* is one of the most powerful tools, where the constituents of the systems are regarded as nodes and the interactions between the nodes as links. Since it has been detected that networks representing real-world systems exhibit small-world properties [3, 4] and scale free (heterogeneous) properties [5] in general, various topological characteristics have been demonstrated and salient results have been reported [6–9]. One of the most important properties of a network is its robustness, that is, its tolerance to the malfunction of some nodes and/or links, which is frequently evaluated as an aggregated property, characterized as the structural phase transition of the emergence of a giant component (GC) [10]. Although vast studies have been conducted in this field, research remains insufficient, because in most studies network patterns were projected as a single layer and the effect exerted by the fact that real-world systems couple with one another was not realized.

For the purposes of analyzing real-world networks more essentially, the concept of *multilayer networks* was developed and is considered a new paradigm of complex network science [11–28]. The seminal work on multilayer networks is the analysis of the robustness of interdependent networks presented in [29, 30]. A mutually connected GC (MCGC) consisting of nodes that belong to a GC in each of all the layers collapses even if only a portion of the nodes has initially failed in one layer, triggering a chain of failures (called the cascade phenomenon) that spreads over all networks. This type of model may in fact be the most dependable because real-world systems in general are becoming increasingly dependent on one another [31].

A different class of multiplex networks consists of those that couple with each other with antagonistic interlayer interactions, which are called antagonistic networks. Several papers were published with regard to robustness of antagonistic networks with neutral degree-degree correlations [32–34]. The theoretical framework was presented for analyzing the robustness on duplex antagonistic networks without initial failures in [32] and later extended to include the failures in [11]. Although it was of surprise

* watanabe@sp.dis.titech.ac.jp
† kaba@c.titech.ac.jp

that these models exhibited the first order transition in the GC size, the definition of the antagonistic property of interlinks was artificial to some extent, in particular for numerical experiments. In our model the property of interlinks is defined simply at microscopic level: nodes that belong to the GC deactivate their replica nodes, while the other nodes, which do not belong to the GC, activate their replica nodes. In addition, we explicitly define that initial failures occur in layer α.

Although our model is defined in a somewhat abstract manner, one may be able to regard it as a family of graph models for ecological systems [35–39]. Employing duplex networks instead of a single network, we represent habitat patches of two categories of species (endangered species and the invasive ones) and interactions in and between them; the habitats of endangered species and those of invaders are projected on layer α and layer β respectively and the GC in each layer represents the largest and most significant habitat of the relevant layer. Each interlayer link represents the antagonistic interaction because the invaders prey on the endangered species, while the latter are conserved, thus eradication program expels the former.

In this paper, we analyze the resilience of antagonistic duplex networks that suffer from failures, in terms of the following three factors: (i) the type of the initial failures; (ii) the remaining effect of the initial failures; and (iii) degree-degree correlations. Two scenarios are examined featuring the two types of initial node failures in the the first layer α: nodes randomly fail (RFs) or high degree nodes selectively fail, called targeted attacks (TAs). The result of the initial failures propagate to the confronting layer β, which causes node failures at the second stage and the outcome return to the layer α. At the third stage, two possibilities are considered for the remaining effect of the initial damage. In one scenario, which is referred to as the *quenched* setting (Case Q), the effect of the initial damage remains, such that failed nodes cannot become active again. In contrast, in the second scenario, termed the *free* setting (Case F), all the nodes are free of the initial damage, which also implies that the nodes can be reactivated with the aid of replica nodes.

In the above-described realistic scenario, Case F corresponds to the situation in which endangered species can recover, while in Case Q, they cannot even though invaders disappear in the area. In both cases percolation processes exhibit periodic phenomena, which were also reported in different model [34]. In addition, we consider the effects of two types of degree-degree correlations, those between nodes within a layer (intralayer degree-degree correlations) and those between replica nodes (interlayer degree-degree correlations). In general, degrees in real-world networks are correlated [40–42], and therefore, the influence of degree-degree correlations is considered one of the most important topics in the research on multilayer networks [11, 43, 44].

As the main part of this paper, we address the development of an analytical framework based on the cavity method developed in statistical mechanics [45–48], which is categorized as a mean field approach [11, 49, 50], supposing a locally tree-like structure and utilizing Bethe-Peierls approximation. In our framework, we first describe the flow for computing GC size from a microscopic viewpoint, the formulation of which is extended to a macroscopic viewpoint and the expected GC size is analytically evaluated solving a set of self-consistent equations numerically. Unfortunately, the results obtained in this fashion deviate from numerical ones, in particular in Case F. The cause of the discrepancy lies in the assumption of self-averaging property that nodes of the same degree have equivalent statistical property though at each single instance local states of some nodes, which are affected from the hysteresis in the layer, deterministically contribute to global property of the relevant layer, namely GC size. The technique to efface the influence of the hysteresis is implicitly used for robustness analysis of multilayer interdependent networks [11] and antagonistic networks [32]. However, this is not valid in the latter case, unlike the former case: some inactive nodes are regarded active, which may makes some of them belong to the GC, if it exists. Although the fraction of these nodes is almost negligible [51], their existence may significantly influence the critical behavior of the system, namely whether the manner of the percolation transition is continuous [34] or discontinuous [8, 32]. In keeping with the periodic phenomena, we heuristically describe the GC size at the microscopic level and extend it to the macroscopic one, the utility of which is confirmed comparing with the numerical ones. The percolation transition of each layer turns out to be continuous in both Cases Q and F in our model; in particular, that of layer α depends on the first stage and the critical point is determined only by intralayer topologies in layer α. On the other hand, the GC size depends on both interlayer and intralayer correlations, in particular the GC size in layer α exceeds about half of the layer size.

The remainder of this paper is organized as follows. In Sec. II, we present the problem set-up and introduce various notations that are used in our analysis. In Sec. III, we develop an analytical framework for evaluating the robustness on antagonistic networks. In Sec. IV, we examine the accuracy in evaluating the GC size of our methodology. We find discrepancies between theory and experiment for the GC size evaluation particularly in Case F. For resolving this inconsistency, we heuristically improve the developed methodology, which is verified by numerical experiments in Sec. V. In Sec. VI, we discuss the influence of interlayer and intralayer degree-degree correlations on robustness of each layer and suggest the relevance of real world ecological systems that are reported recently. In the final section, we conclude the paper with a summary. The periodic phenomena are reconfirmed by the heuristic and used notations are listed for convenience in Appendix A and B, respectively.

II. MODEL

In this section, we present a brief outline of our model of antagonistic networks consisting of layers (networks) α and β, where the number of nodes in each layer is N. They are generated separately in some initial configuration, where no isolated node exists in either network prior to the failure process.

Our model is seeded by initial damages that destroy a portion of the nodes in layer α, chosen uniformly at random or targeted (selected degree-dependent randomly) with probability $1-q$. As the result of the first stage, a GC may remain in layer α, the order of size of which is typically $O(N)$ (or $O(N^{2/3})$ at the critical point exactly) [1]. We define that nodes that belong to the GC in layer α deactivate their replica nodes in layer β, while all the other nodes that do not belong to the GC activate their replica nodes which causes the failure of nodes in layer β at the second stage, resulting in a GC in layer β that differs from the GC in layer α. Similarly, all the nodes that belong to the GC in layer β deactivate their replica nodes, while the rest of nodes activate their replica nodes. The difference between Cases Q and F corresponds to whether the initial damages remain or not in layer α at the third stage: In Case Q, nodes are affected from both the initial damages and layer β, while in Case F, nodes are free from the initial damage and only affected from layer β.

The organization of this section is as follows. In Sec. II A, we show that the failure process oscillates in both Cases Q and F. In Sec. II B, we provide the bipartite graph representations of the original networks, which are necessary for microscopic analysis in Sec. III A. In Sec. II C, the topologies of each networked layer, degree distribution, and interlayer and intralayer degree-degree correlations are introduced. They are used for macroscopic analysis in Sec. III C.

A. Percolation process

In Fig. 1, we categorize the nodes in each layer into three groups and depict them as the stage elapses, which does not depend on the initial failure type (RFs or TAs) or any degree-degree correlations in and/or between networks.

i) After the $t = 1$ percolation process, the nodes in layer α that constitute a GC make their replica nodes inactive at the start of stage $t = 2$. This guarantees that the nodes in layer α are active at the start of stage $t = 3$. In addition, the network topology is unchanged from stage $t = 1$. Therefore, it is ensured that the nodes belong to the GC after the $t = 3$ percolation process, and repeating this argument concludes that the nodes continue to constitute the GC for ever at stages $t = 5, 7, \ldots$. Accordingly, their replica nodes continue to be in-

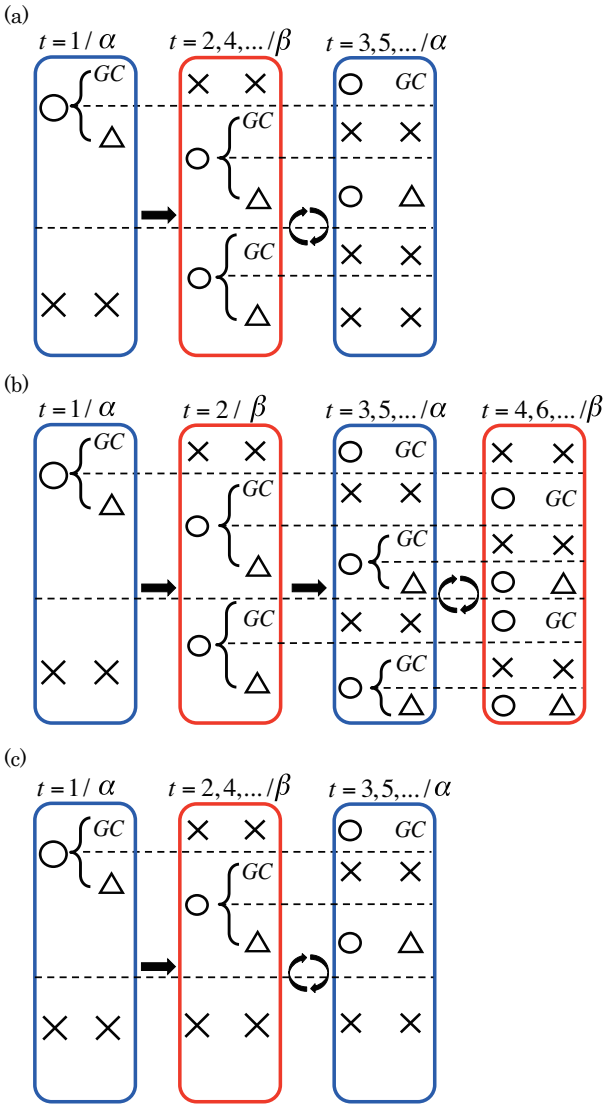

FIG. 1. (Color on-line) Transitions of the states of nodes of the percolation process in antagonistic networks. Each stage is expressed as a large rounded rectangle, where red and blue represent networked layers α and β, respectively. Symbols on the left hand side in a large rectangle express the condition of the set of nodes, and those on the right hand side represent the percolation result under the condition of the left hand side. A cross represents the set of failed nodes at the stage, while a circle represents the set of non-failed nodes, which are classified into two classes: (i) nodes belonging to the GC and (ii) nodes belonging to one of the small components, represented by a triangular shape. Dotted lines separate the groups of nodes that have different percolation results. In Case Q, only the nodes that form the GC affect their replica nodes. In Case F, all nodes influence their replica nodes. (a) and (b) Possible transitions for Cases Q and F, respectively. (c) State transitions realized in the model examined in the case that node i_β is supposed to be the replica node of node i_α [11].

active at stages $t = 2, 4, \ldots$.

ii) The same argument guarantees that the active nodes in layer β at stage $t = 2$ are active at the stages $t = 4, 6, \ldots$, and their replica nodes in α are never reactivated at stages $t = 3, 5, \ldots$.

iii) Statements i) and ii) may appear to guarantee that, when a node has been categorized as inactive, it cannot be reactivated later. However, this is not necessarily the case only in Case F. This is because it is not ensured that the active nodes in layer β at stage $t = 2$, the replica nodes of which in layer α are inactive (damaged or isolated) at stage $t = 1$, form the GC, which allows a portion of the inactive nodes at $t = 1$ to be reactivated at stage $t = 3$.

Consideration of i)–iii) restricts possible state transitions to those depicted in Fig. 1. This figure indicates that we can terminate the repetition of the percolation at stage $t = 3$ in Case Q and at stage $t = 4$ in Case F, considering that the percolation processes converge.

B. Bipartite graph expression and notation

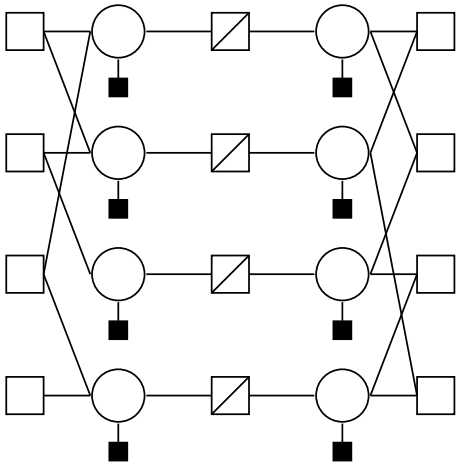

FIG. 2. Diagram of antagonistic duplex networks.

In Fig. 2, we provide the bipartite graph representations of the original networks, which help us consider the message passing scheme in the failure process graphically. Each original node is also a variable node and expressed as a circle. To indicate whether the variable node has initially failed or not without removing it, a function node is connected to each variable node, which is depicted as a black plain square in the figure. For the purpose of passing messages, we append a function node on each interlink and each intralink, respectively. A function node that is depicted as a white square with a slash inside it expresses the role of the interlinks, whereas a function node that is depicted as a white plain square represents the role of the intralink. We now introduce the basic notation for antagonistic bipartite networks. We denote a variable node in layer α by i_α. The variable node i_α is directly connected with the set of function nodes, which is denoted by ∂i_α. We denote a function node on each intralink in layer α by a_α, and we denote a function node on interlinks by p. The function node a_α is directly connected with two variable nodes, denoted as ∂a_α.

C. Statistical expression of graph topologies

One of the most fundamental topologies of network (layer) is degree distribution, which is defined as the probability that a randomly chosen node has degree k_α, denoted by $p_\alpha(k_\alpha)$. We also provide $r_\alpha(k_\alpha)$, which denotes the degree distribution of a link computed as the probability that one terminal node of a randomly chosen link has degree k_α. We describe $r_\alpha(k_\alpha)$ using $p_\alpha(k_\alpha)$:

$$r_\alpha(k_\alpha) = \frac{k_\alpha p_\alpha(k_\alpha)}{\sum_{l_\alpha} l_\alpha p_\alpha(l_\alpha)}. \tag{1}$$

Related to this, the intralayer joint degree distribution (*intralayer degree-degree correlations*) is defined as the probability that, given an intralink is randomly chosen, one terminal node has degree k_α and the second terminal node has degree l_α, which is denoted by $r_\alpha(k_\alpha, l_\alpha)$ and is described using $r_\alpha(k_\alpha)$,

$$r_\alpha(k_\alpha) = \sum_{l_\alpha} r_\alpha(k_\alpha, l_\alpha), \tag{2}$$

Related to the intralayer degree-degree correlations, the intra-joint degree distribution (*intralayer degree-degree correlations*) is described as

$$r_\alpha(k_\alpha|l_\alpha) = \frac{r_\alpha(k_\alpha, l_\alpha)}{r_\alpha(l_\alpha)}, \tag{3}$$

The inter-joint degree distribution is denoted by $P(k_\alpha, k_\beta)$, defined as the probability that the degrees of a randomly chosen node-pair are k_α and k_β, and named *interlayer degree correlations*. The relationship between $p_\alpha(k_\alpha)$ and $P(k_\alpha, k_\beta)$ is

$$p_\alpha(k_\alpha) = \sum_{k_\beta} P(k_\alpha, k_\beta), \tag{4}$$

Related to interlayer joint degree distribution, the inter-conditional distribution is described as

$$P_\alpha(k_\alpha|k_\beta) = \frac{P_\alpha(k_\alpha, k_\beta)}{\sum_{k_\beta} P_\alpha(k_\alpha, k_\beta)}, \tag{5}$$

which is defined as the probability of a node having degree k_α, given that the degree of its replica node is k_β.

Exchanging α with β in Eqs. (1)-(5), we define $r_\beta(k_\beta)$, $r_\beta(k_\beta|l_\beta)$, $p_\beta(k_\beta)$, and $P_\beta(k_\beta|k_\alpha)$, respectively. Using the definition of $P_\beta(k_\beta|k_\alpha)$, the intralayer conditional distributions of *node pairs* are obtained

$$r_\alpha(k_\alpha, k_\beta|l_\alpha, l_\beta) = P_\beta(k_\beta|k_\alpha) r_\alpha(k_\alpha|l_\alpha), \tag{6}$$

the definition of which is the probability that a randomly chosen node pair having the degree (l_α, l_β) is connected with another node pair having the degree (k_α, k_β), given an intralink in layer α.

III. THEORETICAL FRAMEWORK

The aim of this section is to develop a framework for analyzing the robustness of antagonistic networks based on the cavity method. In preparation for evaluating the GC size from the macroscopic viewpoint, we examine the message flow for a single instance from the microscopic viewpoint in Sec. III A; Sec. III A 1 provides the message flow at stages $t = 1$ and $t = 2$, and Sec. III A 2 and Sec. III A 3 describe how the flow behaves for $t \geq 3$ in Cases Q and F, respectively. In Sec. III B, we define macroscopic intralayer messages using microscopic ones. With the aid of local tree approximation and self averaging properties of random network, we extend our formulation to the macroscopic level in Sec. III C; Sec. III C 1 provide the macroscopic message flow at stages $t = 1$ and $t = 2$, and Sec. III C 2 and Sec. III C 3 describe how the macroscopic flow behaves for $t \geq 3$ in Cases Q and F, respectively.

A. Message flow from the microscopic viewpoint

1. First and second stage

We define a binary variable ψ_{i_α}, which is set at 0 or 1 depending on whether or not the node suffers from the initial damage, respectively, and assign it to another variable, named the activity index $s_{i_\alpha}^{t=1}$ of i_α at stage $t = 1$,

$$s_{i_\alpha}^{t=1} \equiv \psi_{i_\alpha}. \tag{7}$$

Note that the total fraction of the active nodes at the initial condition, namely, $\sum_{i_\alpha} \delta\left(\psi_{i_\alpha} = 1\right)/N$, is handled as a survival ratio in Sec. III C. To examine the first stage in layer α, we apply the cavity method presented in [47] for the given set of $\{s_{i_\alpha}^1\}$, which yields a set of self-consistent equations

$$m_{a_\alpha \to i_\alpha}^{t=1} = m_{j_\alpha \to a_\alpha}^{t=1} \quad (\partial a_\alpha = \{i_\alpha, j_\alpha\}), \tag{8}$$

$$m_{i_\alpha \to a_\alpha}^{t=1} = 1 - s_{i_\alpha}^{t=1} + s_{i_\alpha}^{t=1} \prod_{b_\alpha \in \partial i_\alpha \backslash a_\alpha} m_{b_\alpha \to i_\alpha}^{t=1}. \tag{9}$$

Here, $m_{i\to a}^t \in \{0, 1\}$ in general denotes the message from variable node i to function node a at the t-th stage, which takes 0 when i belongs to a GC in the layer from which node a is removed, and unity, otherwise. The message $m_{a\to i}^t \in \{0, 1\}$, on the other hand, conveys 0 from function node a to variable node i at the t-th stage when at least one $j \in \partial a \backslash i$ belongs to the GC, and unity, otherwise. Using the solution of Eqs. (8) and (9), we derive the indices of the GC and the size of the GC in layer α at stage $t = 1$ as

$$\sigma_\alpha^{t=1} = \sum_{i_\alpha} \sigma_{i_\alpha}^{t=1} = \sum_{i_\alpha} s_{i_\alpha}^{t=1} \left(1 - \prod_{a_\alpha \in \partial i_\alpha} m_{a_\alpha \to i_\alpha}^{t=1}\right), \tag{10}$$

which also provides a message from i_α to the function node p on an interlink at stage $t = 1$ as

$$m_{i_\alpha \to p}^{t=1} = \sigma_{i_\alpha}^{t=1} = s_{i_\alpha}^{t=1} \left(1 - \prod_{a_\alpha \in \partial i_\alpha} m_{a_\alpha \to i_\alpha}^{t=1}\right). \tag{11}$$

Because of the antagonistic nature of the interlinks, the inverted value of Eq. (11) is propagated from the function node p to the replica node i_β of layer β after stage $t = 1$ as

$$\begin{aligned} 1 - m_{i_\alpha \to p}^{t=1} &= 1 - s_{i_\alpha}^{t=1} \left(1 - \prod_{a_\alpha \in \partial i_\alpha} m_{a_\alpha \to i_\alpha}^{t=1}\right) \\ &= m_{p \to i_\beta}^{t=2}. \end{aligned} \tag{12}$$

The second stage ($t = 2$) is considered the initial step for layer β. In contrast to the first stage at layer α, a particular set of ψ_{i_β} is not involved (in other words $\psi_{i_\beta} = 1$), because the nodes in layer β are free from the initial damage and influenced only by the activity pattern of layer α provided by the step at stage $t = 1$. The activity index of i_β at the start of stage $t = 2$ is

$$s_{i_\beta}^{t=2} = m_{p \to i_\beta}^{t=2} = 1 - s_{i_\alpha}^{t=1} \left(1 - \prod_{a_\alpha \in \partial i_\alpha} m_{a_\alpha \to i_\alpha}^{t=1}\right). \tag{13}$$

Note that $s_{i_\beta}^{t=2} = 1$ holds, if either $\psi_{i_\alpha} = 0$ or $\psi_{i_\alpha} = 1$ and $\prod_{a_\alpha \in \partial i_\alpha} m_{a_\alpha \to i_\alpha}^{t=1} = 0$ are satisfied. Given $\{s_{i_\beta}^{t=2}\}$, the cavity method provides the self-consistent equations

$$m_{a_\beta \to i_\beta}^{t=2} = m_{j_\beta \to a_\beta}^{t=2} \quad (\partial a_\beta = \{i_\beta, j_\beta\}), \tag{14}$$

$$m_{i_\beta \to a_\beta}^{t=2} = 1 - s_{i_\beta}^{t=2} + s_{i_\beta}^{t=2} \prod_{b_\beta \in \partial i_\beta \backslash a_\beta} m_{b_\beta \to i_\beta}^{t=2}. \tag{15}$$

The solution of Eqs. (14) and (15) provides the GC size of layer β at stage $t = 2$ as

$$\sigma_\beta^{t=2} = \sum_{i_\beta} \sigma_{i_\beta}^{t=2} = \sum_{i_\beta} s_{i_\beta}^{t=2} \left(1 - \prod_{a_\beta \in \partial i_\beta} m_{a_\beta \to i_\beta}^{t=2}\right). \tag{16}$$

The solution also provides the messages from i_β to p and the message from p to i_α as

$$m_{i_\beta \to p}^{t=2} = s_{i_\beta}^{t=2} \left(1 - \prod_{a_\beta \in \partial i_\beta} m_{a_\beta \to i_\beta}^{t=2}\right). \tag{17}$$

$$m_{p \to i_\alpha}^{t=3} = 1 - m_{i_\beta \to p}^{t=2}. \tag{18}$$

At the third and further stages, nodes in layer α receive the inter-messages that are represented as Eq. (18).

2. Third and further stages in Case Q

As already discussed in Sec. II A, we obtain the final robustness of layer α and layer β, which is the robustness of layer α at the first stage (Eq. (10)) and that of layer β at the second stage in (Eq. (16)), respectively.

$$\sigma_{i_\alpha}^{2t'+1} = \sigma_{i_\alpha}^{t=1}, \sigma_{i_\beta}^{2t'} = \sigma_{i_\beta}^{t=2}(\mathrm{Q}). \tag{19}$$

3. Third and further stages in Case F

In Case F, nodes in layer α at stage $t = 3$ are influenced by only interlayer messages and are free from the initial activity indexes, which provides the activity index of i_α as

$$\begin{aligned} s_{i_\alpha}^{t=3}(\mathrm{F}) &= m_{p\to i_\alpha}^{t=3} \\ &= 1 - s_{i_\beta}^{t=2}\left(1 - \prod_{a_\beta \in \partial i_\beta} m_{a_\beta \to i_\beta}^{t=2}\right) \end{aligned} \tag{20}$$

Substituting $s_{i_\alpha}^{t=3}(\mathrm{F})$ for $s_{i_\alpha}^{t=1}$ in Eqs. (8) and (9),

$$m_{a_\alpha \to i_\alpha}^{t=3} = m_{j_\alpha \to a_\alpha}^{t=3} \quad (\partial a_\alpha = \{i_\alpha, j_\alpha\}), \tag{21}$$

$$m_{i_\alpha \to a_\alpha}^{t=3} = 1 - s_{i_\alpha}^{t=3}(\mathrm{F}) + s_{i_\alpha}^{t=3}(\mathrm{F}) \prod_{b_\alpha \in \partial i_\alpha \setminus a_\alpha} m_{b_\alpha \to i_\alpha}^{t=3}, \tag{22}$$

we obtain the solution $m_{a_\alpha \to i_\alpha}^{t=3}$, which derives the size of the GC in layer α as

$$\sigma_\alpha^{t=3} = \sum_{i_\alpha} \sigma_{i_\alpha}^{t=3} = \sum_{i_\alpha} s_{i_\alpha}^{t=3}(\mathrm{F})\left(1 - \prod_{a_\alpha \in \partial i_\alpha} m_{a_\alpha \to i_\alpha}^{t=3}\right) \tag{23}$$

We describe $s_{i_\alpha}^{t=4}(\mathrm{F})$ that denotes the message through the interlink, which each of i_β receives at stage $t = 4$, as

$$\begin{aligned} s_{i_\alpha}^{t=4}(\mathrm{F}) &= m_{p\to i_\beta}^{t=4} = m_{i_\alpha \to p}^{t=3} = 1 - \sigma_{i_\alpha}^{t=3} \\ &= 1 - s_{i_\beta}^{t=3}(\mathrm{F})\left(1 - \prod_{a_\beta \in \partial i_\beta} m_{a_\beta \to i_\beta}^{t=3}\right). \end{aligned} \tag{24}$$

As discussed in Sec. II A, the percolation result at stage $t = 4$ becomes identical to that at stage $t = 2$ in Case F. Therefore, we can determine the indices of each node in each network as

$$\sigma_{i_\alpha}^{2t'+1} = \sigma_{i_\alpha}^{t=3}, \sigma_{i_\beta}^{2t'} = \sigma_{i_\beta}^{t=2}(\mathrm{F}). \tag{25}$$

Consequently, we can terminate the repetition of the percolation at stage $t = 2$ considering the networks converged (Fig. 1 (a)).

The local message flows are categorized with the aid of the bipartite graph expression that is introduced in Sec. II B (See Fig. 3).

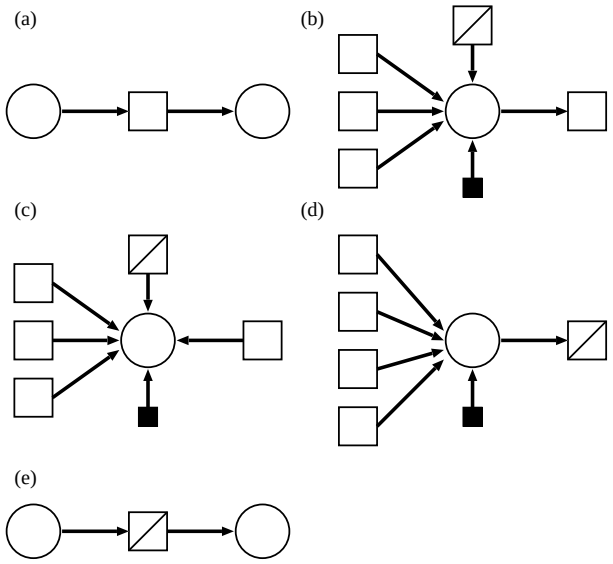

FIG. 3. Diagram of message passing.

(a) The message flow passing a function node in a layer, which corresponds to Eq. (8), Eq. (14) and Eq. (21).

(b) The message flow passing a variable node in a layer, which corresponds to Eq. (9), Eq. (15) and Eq. (22).

(c) The message flow for computing the size of the GC, which corresponds to Eq. (10), Eq. (16), and Eq. (23).

(d) The message flow from a variable node in a layer to a function node on an interlink, which corresponds to Eq. (11) and Eq. (17).

(e) The message flow from a function node on an interlink to a variable node in the layer, which corresponds to Eq. (12) or Eq. (18).

B. Cross link from the microscopic viewpoint to the macroscopic one

We first focus on a node pair i_α and i_β, the degrees of which are l_α and l_β, respectively. The node i_α is initially attached $s_{i_\alpha}^{t=1}$, which is described as Eq. (7). Using $s_{i_\alpha}^{t=1}$, we evaluate $q_{l_\alpha l_\beta}^{\alpha,t=1}$, which denotes the fraction of the *set* of node pairs, the degrees of which are l_α and l_β, taking the value of unity at the first stage:

$$q_{l_\alpha,l_\beta}^{\alpha,t=1} = \frac{\sum_{i_\alpha} \delta\left(|\partial i_\alpha| = l_\alpha\right) \delta\left(|\partial i_\beta| = l_\beta\right) s_{i_\alpha}^{\alpha,t=1}}{\sum_{i_\alpha} \delta\left(|\partial i_\alpha| = l_\alpha\right) \delta\left(|\partial i_\beta| = l_\beta\right)}. \tag{26}$$

In the case of layer β, we denote the relevant active probability by

$$q_{l_\alpha,l_\beta}^{\beta,t=2} = \frac{\sum_{i_\beta} \delta\left(|\partial i_\alpha| = l_\alpha\right) \delta\left(|\partial i_\beta| = l_\beta\right) s_{i_\beta}^{\beta,t=2}}{\sum_{i_\beta} \delta\left(|\partial i_\alpha| = l_\alpha\right) \delta\left(|\partial i_\beta| = l_\beta\right)}. \tag{27}$$

As in Eq. (26), we implicitly define $q_{l_\alpha,l_\beta}^{\alpha,t=3}$ using $s_{i_\alpha}^{\alpha,t=3}$, which leads to Eq. (39). We compute the fraction of mes-

sage $m^{t=1}_{j_\alpha \to a_\alpha} = m^{t=1}_{a_\alpha \to i_\alpha}$ taking unity, which is characterized by the degree of i_α and its replica node i_β, solving the relevant cavity equations (*e.g.*, Eq. (33)) iteratively. We denote the macroscopic message by $I^{\alpha,t=1}_{l_\alpha,l_\beta}$:

$$I^{\alpha,t=1}_{l_\alpha,l_\beta} = \frac{\sum_{i_\alpha} \delta\left(|\partial i_\alpha| = l_\alpha\right) \sum_{a_\alpha \in \partial i_\alpha} m^{\alpha,t=1}_{a_\alpha \to i_\alpha}}{l_\alpha \sum_{i_\alpha} \delta\left(|\partial i_\alpha| = l_\alpha\right) \delta\left(|\partial i_\beta| = l_\beta\right)}. \quad (28)$$

Similarly, in layer β,

$$I^{\beta,t=2}_{l_\alpha,l_\beta} = \frac{\sum_{i_\beta} \delta\left(|\partial i_\beta| = l_\beta\right) \sum_{a_\beta \in \partial i_\beta} m^{\beta,t=2}_{a_\beta \to i_\beta}}{l_\beta \sum_{i_\beta} \delta\left(|\partial i_\alpha| = l_\alpha\right) \delta\left(|\partial i_\beta| = l_\beta\right)}. \quad (29)$$

Note that these macroscopic variables are relevant for network ensembles, and thus, may not be appropriate for each individual network; in particular, each active label of all the nodes is strongly correlated with the network connectivity.

C. Message flow from the macroscopic viewpoint

1. First and second stage

Let us consider the initial stage ($t = 1$) in layer α. First, we set only one parameter q as the initial survival probability, that is, the fraction of non-failed nodes in layer α. In the case of RFs, we set

$$q^{\alpha,t=1}_{k_\alpha,k_\beta} = q^{\alpha,t=1}_{k_\alpha} = q, \quad (30)$$

On the other hand, in the case of TAs, nodes having larger degrees in layer α are preferentially damaged. We therefore set

$$q^{\alpha,t=1}_{k_\alpha,k_\beta} = q^{\alpha,t=1}_{k_\alpha} \begin{cases} 0 & (k_\alpha > \Theta) \\ \Delta & (k_\alpha = \Theta), \\ 1 & (k_\alpha < \Theta) \end{cases} \quad (31)$$

where Θ and Δ are uniquely determined so that

$$q = \sum_{l_\beta} \left(\Delta P(\Theta, l_\beta) + \sum_{l_\alpha < \Theta} P(l_\alpha, l_\beta) \right) \quad (32)$$

holds. Substituting $q^{\alpha,t=1}_{k_\alpha,k_\beta}$ in the self-consistent equation

$$I^{\alpha,t=1}_{l_\alpha,l_\beta} = \sum_{k_\alpha,k_\beta} r_\alpha\left(k_\alpha, k_\beta | l_\alpha, l_\beta\right) \left(1 - q^{\alpha,t=1}_{k_\alpha,k_\beta} + q^{\alpha,t=1}_{k_\alpha,k_\beta} \left(I^{\alpha,t=1}_{k_\alpha,k_\beta}\right)^{k_\alpha - 1}\right), \quad (33)$$

which corresponds to Eqs. (8) and (9). Solving Eq. (33) iteratively, the solution $I^{\alpha,t=1}_{l_\alpha,l_\beta}$ is determined, which offers the fraction of GC in layer α at stage $t = 1$

$$\mu^{t=1}_\alpha = \sum_{k_\alpha,k_\beta} P\left(k_\alpha, k_\beta\right) q^{\alpha,t=1}_{k_\alpha,k_\beta} \left(1 - \left(I^{\alpha,t=1}_{k_\alpha,k_\beta}\right)^{k_\alpha}\right). \quad (34)$$

Let us consider the second stage in layer β, in which $q^{\beta,t=2}_{k_\alpha,k_\beta}$ denotes the probability that nodes do not fail at stage $t = 2$, the degree of which is k_β; their replica node's degree is k_α. Considering the message flow (Eq.(11), Eq. (12), and Eq. (13)), $q^{\beta,t=2}_{k_\alpha,k_\beta}$ is directly calculated from the solution $I^{\alpha,t=1}_{l_\alpha,l_\beta}$ in Eq. (33) as

$$q^{\beta,t=2}_{k_\alpha,k_\beta} = 1 - q^{\alpha,t=1}_{k_\alpha,k_\beta} + q^{\alpha,t=1}_{k_\alpha,k_\beta} \left(I^{\alpha,t=1}_{k_\alpha,k_\beta}\right)^{k_\alpha}. \quad (35)$$

Substituting $q^{\beta,t=2}_{k_\alpha,k_\beta}$ in the self-consistent equation

$$I^{\beta,t=2}_{l_\alpha,l_\beta} = \sum_{k_\alpha,k_\beta} r_\beta\left(k_\alpha, k_\beta | l_\alpha, l_\beta\right) \left(1 - q^{\beta(\mathrm{F}),t=2}_{k_\alpha,k_\beta} + q^{\beta(\mathrm{F}),t=2}_{k_\alpha,k_\beta} \left(I^{\beta,t=2}_{k_\alpha,k_\beta}\right)^{k_\beta - 1}\right), \quad (36)$$

based on Eqs. (14) and (15), we compute the set of messages $I^{\beta,t=2}_{l_\alpha,l_\beta}$, which offers the fraction of the GC in layer β at stage $t = 2$ as

$$\mu^{t=2}_\beta = \sum_{k_\alpha,k_\beta} P\left(k_\alpha, k_\beta\right) q^{\beta,t=2}_{k_\alpha,k_\beta} \left(1 - \left(I^{\beta,t=2}_{k_\alpha,k_\beta}\right)^{k_\beta}\right). \quad (37)$$

2. Third and further stages in Case Q

In Sec. II A, we already discussed that the final GC in layer α is identical to that at stage $t = 1$, while the final GC in layer β is identical to that at stage $t = 2$, which provides

$$\mu_\alpha = \mu^{t=1}_\alpha, \mu_\beta = \mu^{t=2}_\beta. \quad (38)$$

3. Third and further stages in Case F

Here, we naively compute $q^{\alpha(\mathrm{F}),t=3}_{k_\alpha,k_\beta}$, the fraction of nodes that are not failed at stage $t = 3$, based on Eq. (20)

$$q^{\alpha(\mathrm{F}),t=3}_{k_\alpha,k_\beta} = 1 - q^{\beta,t=2}_{k_\alpha,k_\beta} + q^{\beta,t=2}_{k_\alpha,k_\beta} \left(I^{\beta,t=2}_{k_\alpha,k_\beta}\right)^{k_\beta}. \quad (39)$$

As discussed in Sec. IV, it is necessary to evaluate Eq. (20) in detail. Substituting $q^{\alpha(\mathrm{F}),t=3}_{k_\alpha,k_\beta}$ in the self-consistent equation based on Eqs. (21) and (22)

$$I^{\alpha,t=3}_{l_\alpha,l_\beta} = \sum_{k_\alpha,k_\beta} r_\alpha\left(k_\alpha, k_\beta | l_\alpha, l_\beta\right) \left(1 - q^{\alpha(\mathrm{F}),t=3}_{k_\alpha,k_\beta} + q^{\alpha(\mathrm{F}),t=3}_{k_\alpha,k_\beta} \left(I^{\alpha,t=3}_{k_\alpha,k_\beta}\right)^{k_\alpha}\right), \quad (40)$$

we obtain a solution of $I^{\alpha,t=3}_{k_\alpha,k_\beta}$, which yields the fraction of the GC in layer α

$$\mu^{t=3}_\alpha = \sum_{k_\alpha,k_\beta} P\left(k_\alpha, k_\beta\right) q^{\alpha(\mathrm{F}),t=3}_{k_\alpha,k_\beta} \left(1 - \left(I^{\alpha,t=3}_{k_\alpha,k_\beta}\right)^{k_\alpha}\right)$$

(41)

The GC in layer β at stage $t = 4$ is identical to that at stage $t = 2$, which means that the percolation process is only the repetition of the stage at stage $t = 3$ and the stage at stage $t = 4$ alternately. Therefore, the robustness of layer α and layer β is evaluated as

$$\mu_\alpha(\mathrm{F}) = \mu_\alpha^{\mathrm{t}=3}(\mathrm{F}), \mu_\beta(\mathrm{F}) = \mu_\beta^{\mathrm{t}=2}(\mathrm{F}), \tag{42}$$

respectively.

IV. NUMERICAL TEST

A. Procedure

We conducted numerical experiments to confirm the validity of the developed method for analyzing the robustness of antagonistic networks. Here, the procedure of the numerical experiments is briefly described.

(1) We constructed two random networks (layers) α and β, the size of each of which was $N = 10000$. The degree distribution of each layer was represented by $P_\alpha(4) = P_\beta(4) = 0.5, P_\alpha(6) = P_\beta(6) = 0.5$.

(2) To introduce intralayer degree-degree correlations, we set a Pearson coefficient in each layer, C_α and C_β, respectively. For each layer, we randomly selected two pairs of connected nodes and rewired the intralinks, employing the algorithm in [40].

(3) To introduce interlayer degree-degree correlations, we set a Pearson coefficient between layers, C_I. We rewired the interlinks, reordering the indices of one layer. Note that it is necessary to suppose that $P(k_\alpha = x, k_\beta = y) = P(k_\alpha = y, k_\beta = x)$, because C_I does not determine $P(k_\alpha, k_\beta)$ uniquely.

(4) For the degree-correlated networks, we applied the Monte Carlo simulation described below. Setting an initial survival probability q, we chose initially failed nodes randomly depending on the type of failures (RFs or TAs). Failed nodes cause networks to decompose into connected components, each of which is detected using the algorithm in [52, 53]. Note that we modified the open MATLAB code in [53] very slightly in the part of "case 4c ii", tracing the nest of "NodeLP(N)" *sufficiently* to reach its source such that "NodeLPmin" should be put the least cluster label. We terminated the single instance if each active label of all nodes in layer α accorded with that at the last stage in a one-to-one manner. Similar procedures were tested 50 times at each initial survival probability, q.

B. Methodological accuracy

1. Case Q

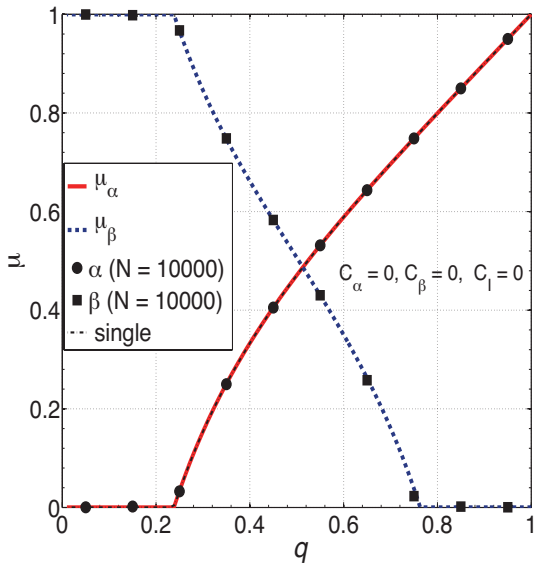

FIG. 4. (Color on-line) Analytical results of the robustness of layer α versus q for the case where antagonistic networks suffer from RFs and the setting is Case Q. Examples of robustness of layer α at stage $t = 1$ are also plotted, which are the results of failure processes that are completed in the single layer α. Each dot is averaged 50 times, produced by numerical experiments.

Fig. 4 shows a comparison of the theoretical prediction obtained for the analysis and the experimental results, which exhibits an excellent consistency. In particular, antagonistic interlinks do not affect the robustness in layer α, which is the GC at stage $t = 1$.

2. Case F

Fig. 5 shows a comparison of the theoretical predictions of the robustness of layers α and β and the numerical results in the condition of Case F. Experimental data for layer β exhibit excellent accordance with the theoretical predictions. However, with regard to the robustness in layer α, there exist significant discrepancies between the theoretical predictions and the numerical results.

V. ACCURACY IMPROVEMENT

The results in Sec. IV indicate that there are significant discrepancies in the GC size evaluation between theory and experiment for Case F. The purpose of this sec-

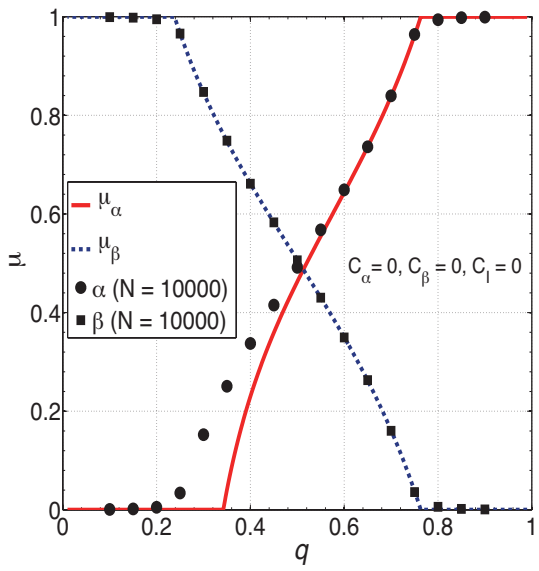

FIG. 5. Analytical results of the robustness of layer α versus q for the case where the antagonistic networks suffer from RFs and the setting is Case F. Each dot is averaged 50 times, produced by numerical experiments.

tion is to resolve this inconsistency. In Sec. V A, we examine the cause of the discrepancies. To improve the accuracy of the theoretical evaluation, we derive alternative expressions for the microscopic Eqs. (20)-(23) and corresponding macroscopic Eqs. (39)-(41). Consequently, we introduce a heuristic treatment in the microscopic level in Sec. V B and extend it to derive macroscopic expressions in Sec. V C, the utility of which is verified by numerical experiments.

A. Clarifying the cause of the discrepancy

The causes of the above discrepancies between theory and experiment lie in the transformation from microscopic variables to macroscopic ones at stage $t = 3$. To reach this resolution, we dissect the GC at stage $t = 3$, which is constitutively heterogeneous and divided into three subsets depending on the history of nodes.

(I) Nodes that belonged to the GC at stage $t = 1$. They necessarily belonged to the GC at stage $t = 3$, which implies that there existed strong correlations between $s_{i_\alpha}^{t=3}$ and $\prod_{a_\alpha \in \partial i_\alpha} m_{a_\alpha \to i_\alpha}^{t=3}$ and thus $q_{k_\alpha,k_\beta}^{\alpha(\mathrm{F}),t=3}$ and $I_{k_\alpha,k_\beta}^{\alpha,t=3}$. Note that the last statement holds if and only if node i_α is classified as this class.

(II) Nodes that failed at stage $t = 1$. They generally belonged to the GC by themselves.

(III) Nodes that belonged to one of the small components at stage $t = 1$. They belonged to the GC at $t = 3$ with the aid of node(s) of (II).

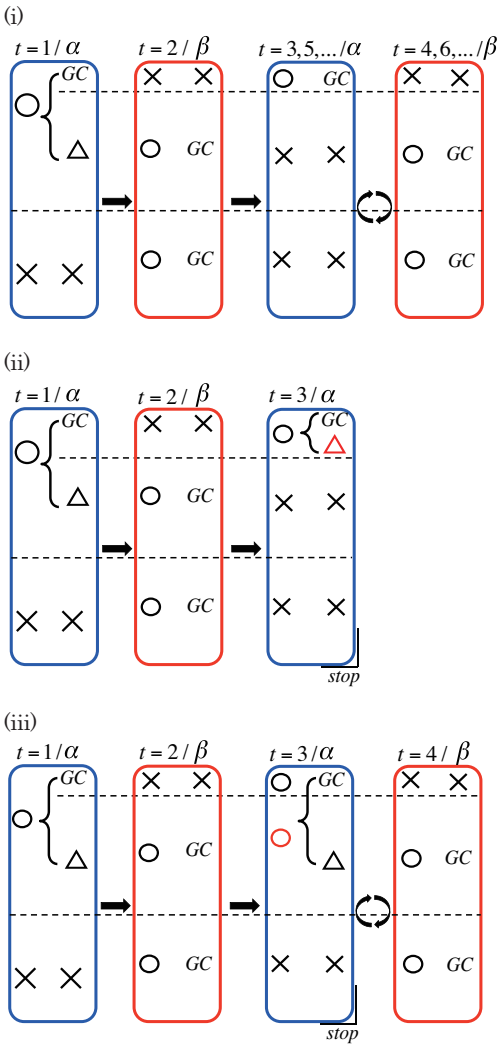

FIG. 6. (Color on-line) Possible transitions for Case F from (i) a microscopic, (ii) a naive macroscopic, and (iii) a modified macroscopic viewpoint. Note that, for simplicity, we considered the situations where the number of active nodes that were isolated from the GC in layer β was *almost negligible*. The meaning of each symbol is similar to that in Fig. 1. The red triangle in (ii) represents the nodes that are not judged constituents of the GC, which causes the discrepancies in Fig. 5. The red circle in (iii) represents the nodes that are actually inactive according to the rule of antagonistic interlinks (see also (i)), but regarded active by dropping the self-feedback term from Eq. (43) as Eq. (44).

Because of these heterogeneity due to the hysteresis, the assumption that nodes of the same degree are statistically equivalent does not hold from the macroscopic viewpoint at stage $t = 3$. Therefore Eq. (41), in which $q_{k_\alpha,k_\beta}^{\alpha(\mathrm{F}),t=3}$ and $I_{k_\alpha,k_\beta}^{\alpha,t=3}$ are independent of each other, underestimate the GC size (See Fig. 6 (i) and (ii)).

In order not to treat the heterogeneity argued above, we drop the term of the past intralayer messages to ob-

$s_{i_\alpha}^{t=1}$	$M_{i_\alpha}^{t=1}$	$M_{i_\alpha}^{t=3}$	$M_{i_\alpha}^{*t=3}$	$s_{i_\alpha}^{t=1}M_{i_\alpha}^{t=1}M_{i_\alpha}^{t=3}$	$s_{i_\alpha}^{t=1}M_{i_\alpha}^{t=1}M_{i_\alpha}^{*t=3}$
1	1	1	1	1	1
1	1	0	0	0	0
1	0	0	0	0	0
1	0	1	1	ϕ	ϕ

TABLE I. All possible cases of $\prod_{a_\alpha\in\partial i_\alpha} m_{a_\alpha\to i_\alpha}^{t=1}$, $\prod_{a_\alpha\in\partial i_\alpha} m_{a_\alpha\to i_\alpha}^{t=3}$, or $\prod_{a_\alpha\in\partial i_\alpha} m_{a_\alpha\to i_\alpha}^{*t=3}$, denoted by $M_{i_\alpha}^{t=1}$, $M_{i_\alpha}^{t=3}$, and $M_{i_\alpha}^{*t=3}$, respectively. ϕ denotes the unrealizable case in which $\prod_{a_\alpha\in\partial i_\alpha} m_{a_\alpha\to i_\alpha}^{t=1}$ vanishes and $\prod_{a_\alpha\in\partial i_\alpha} m_{a_\alpha\to i_\alpha}^{t=3}$ takes a unity at the same time.

scure (or *encapsulate*) the connectivity in the relevant layer in Eq. (20) . Note that unlike interdependent networks, this treatment has a possibility of considering that some of failed nodes belong to the GC in layer α at stage $t=3$ in antagonistic networks, which depends on the percolation result of layer β at stage $t=2$ (See Fig. 7). To compensate this inconsistency, we deduct them using the original interlayer message to derive the GC size at microscopic level.

B. Heuristic

To remain our model analytically tractable, we define the provisional active variables $s_{i_\alpha}^{*t=3}$ instead of $s_{i_\alpha}^{t=3}(\mathrm{F})$, such that they do not include messages in layer α. We first describe Eq. (20) in detail and show that $s_{i_\alpha}^{t=3}(\mathrm{F})$ includes the past intralayer messages in layer α.

$$s_{i_\alpha}^{t=3}(\mathrm{F}) = s_{i_\alpha}^{t=1} + \left(1-s_{i_\alpha}^{t=1}\right)\prod_{a_\beta\in\partial i_\beta} m_{a_\beta\to i_\beta}^{t=2} - s_{i_\alpha}^{t=1}\prod_{a_\alpha\in\partial i_\alpha} m_{a_\alpha\to i_\alpha}^{t=1}\left(1-\prod_{a_\beta\in\partial i_\beta} m_{a_\beta\to i_\beta}^{t=2}\right), \tag{43}$$

It is clear that $s_{i_\alpha}^{t=3}(\mathrm{F})$ is already influenced by the connectivity of layer α, because it includes the term $\prod_{a_\alpha\in\partial i_\alpha} m_{a_\alpha\to i_\alpha}^{t=1}$, which is indeed $\prod_{a_\alpha\in\partial i_\alpha} m_{a_\alpha\to i_\alpha}^{t=3}$ itself in the case that node i_α has the history (I) (see Table I). Supposing the term $\prod_{a_\alpha\in\partial i_\alpha} m_{a_\alpha\to i_\alpha}^{t=1} = 0$ in Eq. (43), we define the provisional active variables,

$$s_{i_\alpha}^{*t=3}(\mathrm{F}) \equiv s_{i_\alpha}^{t=1} + \left(1-s_{i_\alpha}^{t=1}\right)\prod_{a_\beta\in\partial i_\beta} m_{a_\beta\to i_\beta}^{t=2}, \tag{44}$$

Substituting $s_{i_\alpha}^{*t=3}$ for $s_{i_\alpha}^{t=3}(\mathrm{F})$ in Eqs. (21) and (22), we compute the provisional message $m_{a_\alpha\to i_\alpha}^{*t=3}$. Employing $s_{i_\alpha}^{*t=3}$ and $m_{a_\alpha\to i_\alpha}^{*t=3}$ in Eq. (23), we can compute the provisional GC,

$$\sigma_{i_\alpha}^{*t=3} \equiv s_{i_\alpha}^{*t=3}(\mathrm{F})\left(1-\prod_{a_\alpha\in\partial i_\alpha} m_{a_\alpha\to i_\alpha}^{*t=3}\right), \tag{45}$$

the sum of which is larger than actual GC size in particular when the number of isolated nodes in layer β is not negligible (See Fig. 7).

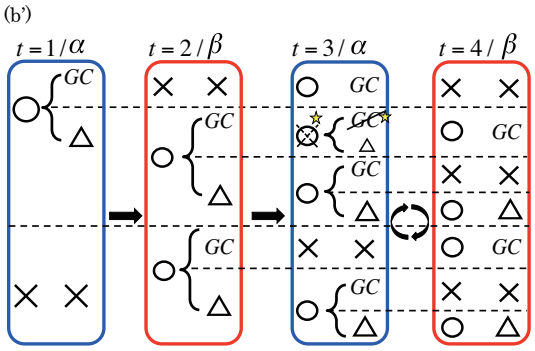

FIG. 7. (Color on-line) Possible transitions from a modified macroscopic viewpoint for Case F in the situations where the number of active nodes that are isolated from the GC in layer β is *not negligible*. Because some initially destroyed nodes in layer α are revived at stage $t=3$ because of antagonistic interlinks, some nodes that are treated as active by encapsulation involuntarily belong to the GC at stage $t=3$, which allows the impossible state transitions that are highlighted by stars. To compensate this inconvenience, we modified the evaluation of the GC size as Eq. (47), highlighted by a small diagonal line. The meaning of each symbol is the same as in Fig. 1.

Our idea is to replace only intralayer messages in Eq. (23): employing $m_{a_\alpha\to i_\alpha}^{*t=3}$ instead of $m_{a_\alpha\to i_\alpha}^{t=3}$, we approximately describe the GC label of each node at stage $t=3$ (Eq. (23)) in detail:

$$\sigma_{i_\alpha}^{t=3}(\mathrm{F}) \approx s_{i_\alpha}^{*t=3}(\mathrm{F})\left(1-\prod_{a_\alpha\in\partial i_\alpha} m_{a_\alpha\to i_\alpha}^{*t=3}\right) - s_{i_\alpha}^{t=1}\prod_{a_\alpha\in\partial i_\alpha} m_{a_\alpha\to i_\alpha}^{t=1} \cdot \left(1-\prod_{a_\beta\in\partial i_\beta} m_{a_\beta\to i_\beta}^{t=2}\right)\left(1-\prod_{a_\alpha\in\partial i_\alpha} m_{a_\alpha\to i_\alpha}^{*t=3}\right), \tag{46}$$

where it is possible to replace $\prod_{a_\alpha\in\partial i_\alpha} m_{a_\alpha\to i_\alpha}^{t=1}\prod_{a_\alpha\in\partial i_\alpha} m_{a_\alpha\to i_\alpha}^{t=3}$ with $\prod_{a_\alpha\in\partial i_\alpha} m_{a_\alpha\to i_\alpha}^{t=3}$, which is due to the correlations between the product of intralayer messages at stage $t=1$ and that at stage $t=3$ (see Table I). Therefore, we renew Eq. (46) as

$$\sigma_{i_\alpha}^{t=3}(\mathrm{F}) \approx \sigma_{i_\alpha}^{*t=3} - s_{i_\alpha}^{t=1}\left(1-\prod_{a_\beta\in\partial i_\beta} m_{a_\beta\to i_\beta}^{t=2}\right) \cdot \left(\prod_{a_\alpha\in\partial i_\alpha} m_{a_\alpha\to i_\alpha}^{t=1} - \prod_{a_\alpha\in\partial i_\alpha} m_{a_\alpha\to i_\alpha}^{*t=3}\right), \tag{47}$$

where the second term of Eq. (47) corresponds to deducting the nodes that incorrectly belong to the GC.

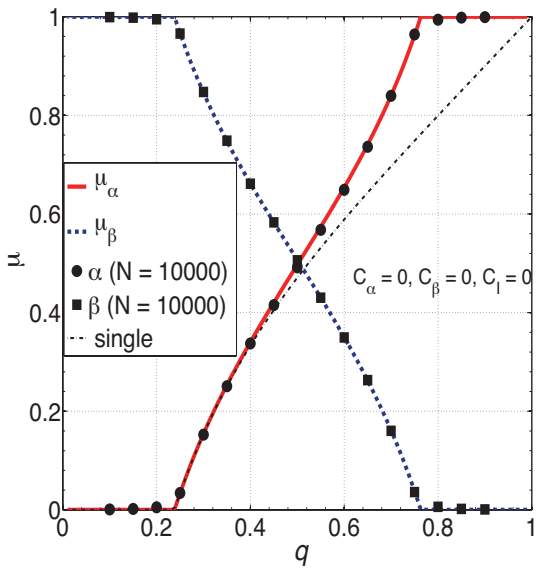

FIG. 8. (Color on-line) Modified analytical results of the robustness of layer α versus q for the case where antagonistic networks suffer from RFs and the setting is Case F. Examples of robustness of layer α at stage $t = 1$ are also plotted, which are the results of failure processes that are completed in the single layer α. Each dot is averaged 50 times, produced by numerical experiments.

C. Macroscopic evaluation and numerical validation

For the purposes of macroscopic analysis, we denote the ratio of active nodes at $t = 3$ based on Eq. (44)

$$q_{k_\alpha,k_\beta}^{*\alpha(\mathrm{F}),t=3} = q_{k_\alpha,k_\beta}^{\alpha,t=1} + \left(1 - q_{k_\alpha,k_\beta}^{\alpha,t=1}\right)\left(I_{k_\alpha,k_\beta}^{\beta,t=2}\right)^{k_\beta}, \quad (48)$$

Substituting $q_{k_\alpha,k_\beta}^{*\alpha(\mathrm{F}),t=3}$ in the self-consistent equation

$$I_{l_\alpha,l_\beta}^{*\alpha,t=3} = \sum_{k_\alpha,k_\beta} r_\alpha\left(k_\alpha,k_\beta|l_\alpha,l_\beta\right) \cdot \left(1 - q_{k_\alpha,k_\beta}^{*\alpha(\mathrm{F}),t=3} + q_{k_\alpha,k_\beta}^{*\alpha(\mathrm{F}),t=3}\left(I_{k_\alpha,k_\beta}^{*\alpha,t=3}\right)^{k_\alpha}\right) \quad (49)$$

we compute the set of messages $I_{l_\alpha,l_\beta}^{*\alpha,t=3}$, which yields the fraction of the GC

$$\mu_{\alpha(\mathrm{F})}^{\star t=3} = \sum_{k_\alpha,k_\beta} P\left(k_\alpha,k_\beta\right) q_{k_\alpha,k_\beta}^{*\alpha(\mathrm{F}),t=3}\left(1 - \left(I_{k_\alpha,k_\beta}^{*\alpha,t=3}\right)^{k_\alpha}\right) - q_{k_\alpha,k_\beta}^{\alpha,t=1}\left(1 - \left(I_{k_\alpha,k_\beta}^{\beta,t=2}\right)^{k_\beta}\right) \cdot \left(\left(I_{k_\alpha,k_\beta}^{\alpha,t=1}\right)^{k_\alpha} - \left(I_{k_\alpha,k_\beta}^{*\alpha,t=3}\right)^{k_\alpha}\right), \quad (50)$$

based on Eq. (47).

Fig. 8 shows the size of the GCs in layer α predicted by Eq. (50) in the case where no degree-degree correlations exist, which excellently accords with the experimental data. As long as we examined, similar accuracy was also achieved for the other parameter sets.

VI. RESULT

A. Influence of degree-degree correlaions

We here argue the influence of interlayer and intralayer degree-degree correlations on the robustness of each layer, the specific topologies of which are defined in IV A. We narrow an argument to the Case F and TAs, because the percolation processes in each layer in Case Q can be reduced to those of a single network and the influence of degree-degree-correlations on robustness in RFs is considerably smaller than that in TAs. In Figs. 9 and 10, we show examples of the robustness of layer α and the effects of various interlayer and intralayer degree-degree correlations.

We focus on the effect of degree-degree correlations on critical (minimum) robustness ($\mu_\alpha \approx 0$) and maximum robustness ($\mu_\alpha \approx 1$) of layer α, respectively. The thresholds at which μ_α vanishes depend on only its intralayer degree-degree correlations, which are characterized with the Pearson coefficient, C_α. This is because the GC at $t = 1$ plays a role of the *core* of the final GC and thus if there exists no GC at $t = 1$, no node can belong to the GC thereafter. On the while, the maximum robustness of layer α is affected from both intralayer degree-degree-correlations and interlayer degree-degree correlations, the transition point of which accords with that for critical robustness of layer β.

Let us consider the advantageous conditions for maximum robustness of layer α, the parameter example of which is $C_\alpha = 0.6, C_\beta = -0.4, C_I = -1$ in Fig. 9. Layer α is more robust against TAs if its degree-degree correlations are positive. In addition, layer α is more robust if layer β is more fragile due to antagonistic properties. Layer β is the most fragile if its intralayer degree-degree correlations are negative and it suffers from TAs, which are realized in the cases where interlayer degree-degree correlations are highly negative. In this case, nodes of higher degree in layer β become inactive because they connect with nodes of lower degree in layer α that are tend to be active due to TAs in layer α.

Considering the above, it is natural that maximum robustness of layer α is the most fragile if the parameter example is $C_\alpha = -0.4, C_\beta = 0.6, C_I = 1$ in Fig. 10, because each sign of the parameter is opposite with that in the conditions that are advantageous for layer α.

B. Possible relevance to real world systems

As for significance to real world systems, the antagonistic networks may serve as a model of complex ecological interactions between endangered species and in-

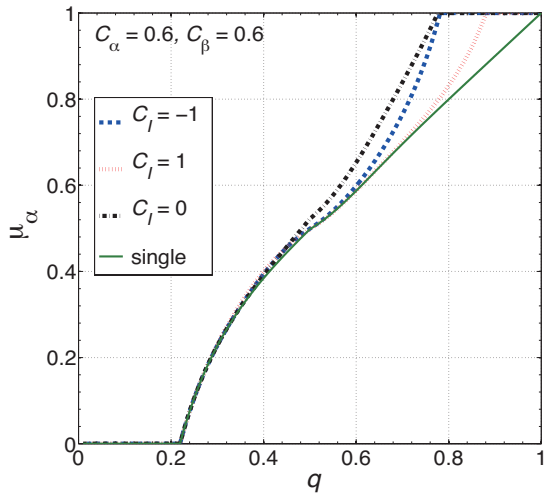

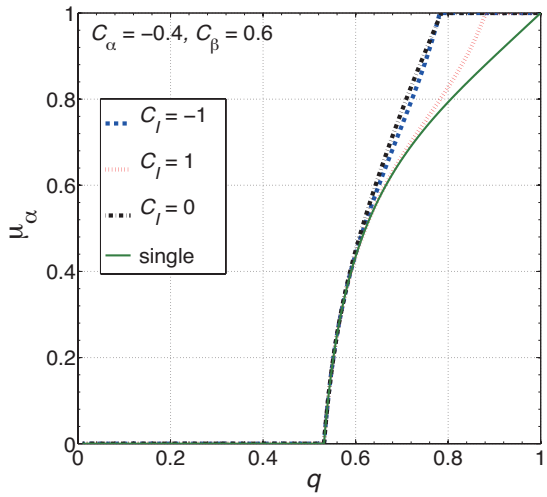

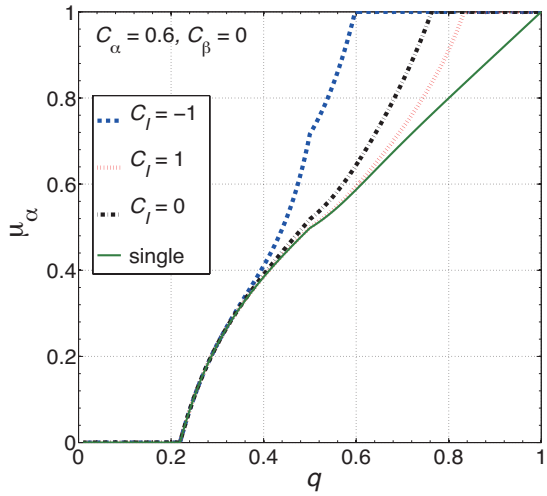

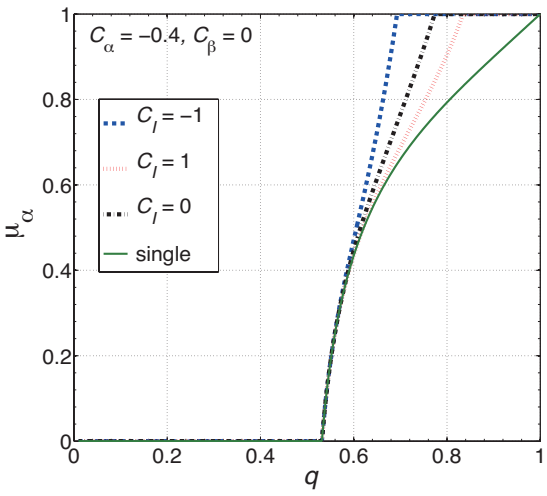

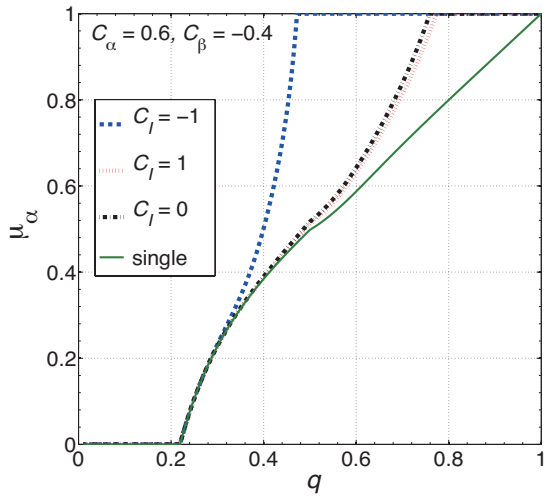

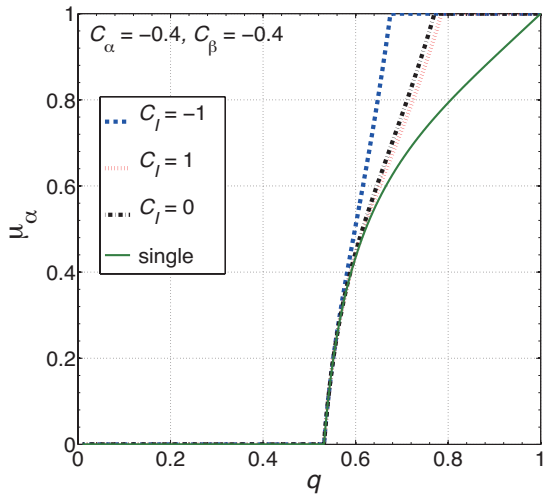

FIG. 9. (Color on-line) GC size in layer α versus the initial parameter q for the case where antagonistic networks suffer from TAs, the remaining effect of which is Case F. The GC size in layer α at stage $t = 1$ is also shown, which is the result of the percolation process that is completed in the single layer α. The intralayer correlations in layer α are fixed to be positive, *e.g.*, $C_\alpha = 0.6$, to focus on the effect of intralayer degree-degree correlations in layer β and interlayer degree-degree correlations on the robustness of layer α.

FIG. 10. (Color on-line) GC size in layer α versus the initial parameter q for the case where antagonistic networks suffer from TAs, the remaining effect of which is Case F. The GC size in layer α at stage $t = 1$ is also shown, which is the result of the percolation process that is completed in a single network. The intralayer correlations in layer α are fixed to be negative, *e.g.*, $C_\alpha = -0.4$, to focus on the effect of intralayer degree-degree correlations in layer β and interlayer degree-degree correlations on the robustness of layer α.

vaders. Refs. [54, 55] report such ecological relationship in the Amami islands in Japan: populations of endangered species, such as the Amami rabbit (*Pentalagus furnessi*) and the Amami Ishikawa's frog (*Odorrana splendida*) were restored to the almost original level at the areas where invaders, such as the small Indian mongoose (*Herpestes auropunctatus*) were exterminated, whereas few were observed in the places where the invaders were established.

Our analysis shows that if initially damaged nodes can be reactivated (Case F), the GC size is restored to the original level owing to the antagonistic inhibition to the replica nodes as long as the fraction of the initial damage is sufficiently small. This is consistent with the above reports. The endangered species in the reports have relatively high reproduction rates and short life cycles, which may fit the condition of Case F. On the other hand, species such as large mammals and primates have low reproduction rates and long life cycles, and may correspond to Case Q, for which populations of the species cannot be restored only by the antagonistic interaction. However, our analysis, in conjunction with Refs. [54, 55], implies that, even in such cases, combination of increasing the reactivation rate of endangered species by human-induced methods such as relocation and extermination of invasive species is an effective scheme for conserving ecological systems.

VII. SUMMARY

In this paper, we developed an analytical methodology based on the cavity method to study the robustness of duplex networks coupled with antagonistic interlinks, considering intralayer and interlayer degree-degree correlations. We investigated two scenarios according to whether initially failed nodes are able to revive (Case F) or not (Case Q) with the aid of their replica nodes. In both Cases Q and F, we showed that the failure process periodically repeated because of the peculiarity of the antagonistic property of interlinks and the percolation transition exhibited continuous. The oscillation was due to hysteresis of each layer, which led to the inconsistency between theory and experiment particularly for Case F. Therefore, we introduced a heuristic treatment for improving the theoretical prediction accuracy, the utility of which was verified by numerical experiments.

We also argued the most advantageous situations for layer α in terms of degree-degree correlations, employing bimodal networks. While the minimum robustness of layer α ($\mu_\alpha \approx 0$) was affected from only intralayer degree-degree correlations in layer α, the maximum robustness of layer α ($\mu_\alpha \approx 1$) was influenced from various degree-degree correlations; the most robust situations are positive intralayer degree-degree correlations in layer α and negative intralayer degree-degree correlations in layer β and negative interlayer degree-degree correlations. As for significance to real world systems, a possible relevance to ecological systems that are composed of endangered and invasive species is mentioned.

Future works include to construct model and analytical framework that works with more realistic settings by network approach.

ACKNOWLEDGMENT

This work was partially supported by KAKENHI No. 25120013 (YK).

Appendix A: Reconfirming the periodicity by the heuristic

Although we already made sure that the percolation processes oscillates in both Cases Q and F in Sec. II A, we here reconfirm these by the heuristic in Sec. V B.

1. Case Q

The active variable of each node at stage $t = 3$ is provided as

$$\begin{aligned} s_{i_\alpha}^{t=3}(\mathrm{Q}) &= s_{i_\alpha}^{t=1} m_{p\to i_\alpha}^{t=3} \\ &= (s_{i_\alpha}^{t=1})^2 + s_{i_\alpha}^{t=1}\left(1 - s_{i_\alpha}^{t=1}\right) \prod_{a_\beta\in\partial i_\beta} m_{a_\beta\to i_\beta}^{t=2} \\ &\quad - (s_{i_\alpha}^{t=1})^2 \prod_{a_\alpha\in\partial i_\alpha} m_{a_\alpha\to i_\alpha}^{t=1}\left(1 - \prod_{a_\beta\in\partial i_\beta} m_{a_\beta\to i_\beta}^{t=2}\right). \\ &= s_{i_\alpha}^{t=1}\left(1 - \prod_{a_\alpha\in\partial i_\alpha} m_{a_\alpha\to i_\alpha}^{t=1}\left(1 - \prod_{a_\beta\in\partial i_\beta} m_{a_\beta\to i_\beta}^{t=2}\right)\right). \end{aligned} \tag{A1}$$

Substituting $m_{a_\alpha\to i_\alpha}^{t=1} = 0$ in Eq. (A1), we obtain $s_{i_\alpha}^{*t=3}(\mathrm{Q}) = s_{i_\alpha}^{t=1}$, which also shows that $m_{a_\alpha\to i_\alpha}^{*t=3}$ is equivalent with $m_{a_\alpha\to i_\alpha}^{t=1}$. Using $s_{i_\alpha}^{*t=3}(\mathrm{Q})$ and $m_{a_\alpha\to i_\alpha}^{*t=3}$, we obtain the result on the GC size, namely

$$\begin{aligned} \sigma_{i_\alpha}^{t=3} &\approx s_{i_\alpha}^{t=3}(\mathrm{Q})\left(1 - \prod_{a_\alpha\in\partial i_\alpha} m_{a_\alpha\to i_\alpha}^{*t=3}\right) \\ &= s_{i_\alpha}^{t=1}\left(1 - \prod_{a_\alpha\in\partial i_\alpha} m_{a_\alpha\to i_\alpha}^{t=1}\right)^2 + \\ &\quad \prod_{a_\alpha\in\partial i_\alpha} m_{a_\alpha\to i_\alpha}^{t=1}\left(1 - \prod_{a_\alpha\in\partial i_\alpha} m_{a_\alpha\to i_\alpha}^{t=1}\right)\prod_{a_\beta\in\partial i_\beta} m_{a_\beta\to i_\beta}^{t=2} \\ &= s_{i_\alpha}^{t=1}\left(1 - \prod_{a_\alpha\in\partial i_\alpha} m_{a_\alpha\to i_\alpha}^{t=1}\right) \\ &= \sigma_{i_\alpha}^{t=1}. \end{aligned} \tag{A2}$$

2. Case F

Substituting Eq. (43) to Eq. (24), we describe $s_{i_\beta}^{t=4}(\mathrm{F})$ in detail,

$$\begin{aligned} s_{i_\beta}^{t=4}(\mathrm{F}) &= 1 - s_{i_\alpha}^{*t=3}\left(1 - \prod_{a_\alpha\in\partial i_\alpha} m_{a_\alpha\to i_\alpha}^{t=3}\right) \\ &\quad + s_{i_\alpha}^{t=1}\left(\prod_{a_\alpha\in\partial i_\alpha} m_{a_\alpha\to i_\alpha}^{t=1} - \prod_{a_\alpha\in\partial i_\alpha} m_{a_\alpha\to i_\alpha}^{t=3}\right) \\ &\quad \cdot \left(1 - \prod_{a_\beta\in\partial i_\beta} m_{a_\beta\to i_\beta}^{t=2}\right). \end{aligned} \tag{A3}$$

Note that $\prod_{a_\alpha\in\partial i_\alpha} m_{a_\alpha\to i_\alpha}^{t=1} \prod_{a_\alpha\in\partial i_\alpha} m_{a_\alpha\to i_\alpha}^{t=3}$ is replaced with $\prod_{a_\alpha\in\partial i_\alpha} m_{a_\alpha\to i_\alpha}^{t=3}$ because of Table I. Supposing that $\prod_{a_\beta\in\partial i_\beta} m_{a_\beta\to i_\beta}^{t=2}$ vanishes in Eq. (A3), which also replaces $s_{i_\alpha}^{*t=3}$ with $s_{i_\alpha}^{t=1}$ because of Eq. (44), we define

$$\begin{aligned} s_{i_\beta}^{*t=4}(\mathrm{F}) &\equiv 1 - s_{i_\alpha}^{t=1}\left(1 - \prod_{a_\alpha\in\partial i_\alpha} m_{a_\alpha\to i_\alpha}^{t=3}\right) \\ &\quad + s_{i_\alpha}^{t=1}\left(\prod_{a_\alpha\in\partial i_\alpha} m_{a_\alpha\to i_\alpha}^{t=1} - \prod_{a_\alpha\in\partial i_\alpha} m_{a_\alpha\to i_\alpha}^{t=3}\right) \\ &= 1 - s_{i_\alpha}^{t=1} + s_{i_\alpha}^{t=1}\prod_{a_\alpha\in\partial i_\alpha} m_{a_\alpha\to i_\alpha}^{t=1} \\ &= s_{i_\beta}^{t=2}, \end{aligned} \tag{A4}$$

where the last equal sign is because of Eq. (13). Employing $s_{i_\beta}^{*t=4}(\mathrm{F})$ instead of $s_{i_\beta}^{t=2}$ in Eq. (14) and (15), we derive the provisional message at $t = 4$, $m_{a_\beta\to i_\beta}^{*t=4}$, which completely accords with $m_{a_\beta\to i_\beta}^{t=2}$ because of Eq. (A4).

The label of the GC at $t = 4$ is derived using the original interlayer message $s_{i_\beta}^{t=4}(\mathrm{F})$ and the provisional message $m_{a_\beta\to i_\beta}^{*t=4}$. Namely,

$$\begin{aligned} \sigma_{i_\beta}^{t=4} &\approx s_{i_\beta}^{t=4}(\mathrm{F})\left(1 - \prod_{a_\beta\in\partial i_\beta} m_{a_\beta\to i_\beta}^{*t=4}\right) \\ &= s_{i_\beta}^{t=4}(\mathrm{F})\left(1 - \prod_{a_\beta\in\partial i_\beta} m_{a_\beta\to i_\beta}^{t=2}\right) \\ &= s_{i_\alpha}^{t=2}\left(1 - \prod_{a_\beta\in\partial i_\beta} m_{a_\beta\to i_\beta}^{t=2}\right) \\ &\quad - \left(1 - s_{i_\alpha}^{t=1}\right)\left(1 - \prod_{a_\alpha\in\partial i_\alpha} m_{a_\alpha\to i_\alpha}^{t=3}\right) \\ &\quad \cdot \prod_{a_\beta\in\partial i_\beta} m_{a_\beta\to i_\beta}^{t=2}\left(1 - \prod_{a_\beta\in\partial i_\beta} m_{a_\beta\to i_\beta}^{t=2}\right) \\ &= \sigma_{i_\beta}^{t=2}, \end{aligned} \tag{A5}$$

where the last equal sign is derived because $\prod_{a_\beta\in\partial i_\beta} m_{a_\beta\to i_\beta}^{t=2}\left(1 - \prod_{a_\beta\in\partial i_\beta} m_{a_\beta\to i_\beta}^{t=2}\right)$ always vanishes. We also note that the label of the provisional GC, which is defined as $\sigma_{i_\beta}^{*t=4} \equiv s_{i_\beta}^{*t=4}(\mathrm{F})\left(1 - \prod_{a_\beta\in\partial i_\beta} m_{a_\beta\to i_\beta}^{*t=4}\right) = \sigma_{i_\beta}^{t=2}$, also correctly evaluates the GC at $t = 4$, because there exist no nodes that incorrectly belong to the GC at $t = 4$ even if we set $s_{i_\beta}^{*t=4}(\mathrm{F})$ instead of $s_{i_\beta}^{t=4}(\mathrm{F})$.

Appendix B: Notations

Indice	Definitions or meanings
α, β	Layer α and layer β, respectively.
a_α	Index of a function node on a link in layer α.
i_α, j_α	Index of a node (variable node) in layer α.
p	Index of a function node on an interlink.
∂i_α	Set of nodes in layer α that connect with node i_α.
$\lvert\partial i_\alpha\rvert$	Degree of node i_α.
k_α, l_α	Degree of a node in layer α.
$P(k_\alpha, k_\beta)$	Interlayer joint degree distribution.
$r_\alpha(k_\alpha)$	Distribution of the degree of a node in one terminal, given a randomly chosen intralink in layer α.
$r_\alpha(k_\alpha, k_\beta \lvert l_\alpha, l_\beta)$	Conditional interlayer degree-degree distribution.
C_α, C_β, C_I	Pearson coefficients in layer α, layer β, and between layers, respectively.
Case Q, Case F	Remaining effect of the initial failure is quenched and free, respectively.
ψ_{i_α}	Binary variable that represents whether a node i_α initially fails ($\psi_{i_\alpha}=0$) or not ($\psi_{i_\alpha}=1$).
$s_{i_\alpha}^{2t'-1}$	Binary variable that represents whether a node i_α fails ($s_{i_\alpha}^{2t'-1}=0$) or not ($s_{i_\alpha}^{2t'-1}=1$) at the onset of the stage $2t'-1$.
$m_{a_\alpha\to i_\alpha}^{2t'-1}$	Message that propagates from function node a_α to (variable) node i_α at stage $2t'-1$, where $\partial a_\alpha = \{i_\alpha, j_\alpha\}$. If node j_α belongs to the GC on i_α-cavity system, $m_{a\to i_\alpha}^{2t'-1}=0$ is completed; otherwise $m_{a\to i_\alpha}^{2t'-1}=1$ is completed.
$\sigma_{i_\alpha}^{2t'-1}$	Binary variable that represents whether node i_α belongs to the GC in layer α ($\sigma_{i_\alpha}^{2t'-1}=1$) or not ($\sigma_{i_\alpha}^{2t'-1}=0$) at stage $2t'-1$.
q	Fraction of (variable) nodes that are active (in other words, have not failed) at the onset of the initial stage.
$q_{k_\alpha,k_\beta}^{\alpha,2t'-1}$	Active probability of (variable) nodes in layer α at the onset of the stage $2t'-1$, the degrees of which are k_α; the degrees of its replica nodes are k_β.
$I_{l_\alpha,l_\beta}^{\alpha,t=1}$	Message on an intralink in layer α at stage $t=1$ from the macroscopic viewpoint, which is defined in Eq. (28).
$\mu_\alpha^{2t'-1}$	Expected GC size in layer α at the end of stage $2t'-1$.

[1] P. Erdös and A. Réyni, Publ. Math. **6**, 290 (1959).
[2] B. Bollobás, S. Janson, and O. Riordan, Random Struct. Alg. **31**, 3 (2007).
[3] S. H. Strogatz, Nature **410**, 268 (2001).
[4] D. J. Watts, *Small Worlds: The Dynamics of Networks between Order and Randomness* (Princeton University Press, Princeton, NJ, 1999).
[5] R. Albert and A.-L. Barabási, Rev. Mod. Phys. **74**, 47 (2002).
[6] M. E. J. Newman, SIAM Rev. **45**, 167 (2003).
[7] S. N. Dorogovtsev and J. F. F. Mendes, Adv. Phys. **51** 1079 (2002).
[8] S. Boccaletti, V. Latora, Y. Moreno, M. Chavez, and D.-U. Hwang, Phys. Rep. **424**, 175-308 (2006).
[9] M. Barthelémy, Phys. Rep. **499** (2011).
[10] D. S. Callaway, M. E. J. Newman, S. H. Strogatz, and D. J. Watts, Phys. Rev. Lett. **85**, 5468 (2000).
[11] S. Boccaletti, G. Bianconi, R. Criado, C.I. del Genio, J. Gómez-Gardenes, M. Romance, I. Sendina-Nadal, Z. Wang, and M. Zanin, Phys. Rep. **544** (2014).
[12] M. Kivelä, A. Arenas, M. Barthélemy, J.P. Gleeson, Y. Moreno, and M.A. Porter, Journal of Complex Networks
[13] Gregorio ÓAgostino and Antonio Scala, *Networks of Networks: The Last Frontier of Complexity* (Springer, 2014).
[14] J. Gao, S. V. Buldyrev, S. Havlin, and H. E. Stanley, Phys. Rev. Lett. **107**, 195701 (2011).
[15] R. G. Morris and M. Barthelemy, Phys. Lett. **109**, 128703 (2012).
[16] G. J. Baxter, S. N. Dorogovtsev, A. V. Goltsev, and J. F. F. Mendes, Phys. Lett. **109**, 248701 (2012).
[17] S. V. Buldyrev, N. W. Shere, and G. A. Cwilich, Phys. Rev. E **83**, 016112 (2011).
[18] X. Huang, J. Gao, S. V. Buldyrev, S. Havlin, and H. E. Stanley, Phys. Rev. E **83**, 065101 (2011).
[19] Y. Hu, B. Ksherim, R. Cohen, and S. Havlin, Phys. Rev. E **84**, 066116 (2011).
[20] D. Zhou, J. Gao, H. E. Stanley, and S. Havlin, Phys. Rev. E **87**, 052812 (2013).
[21] J. Shao, S.V. Buldyrev, S. Havlin, and H.E. Stanley, Phys. Rev. E **83**, 036116 (2011).
[22] R. Parshani, C. Rozenblat, D. Ietri, C. Ducruet, and S. Havlin, Europhys. Lett. **92**, 68002 (2010).
[23] Z. Wang, A. Szolnoki, and M. Perc, Europhys. Lett. **97**, 48001 (2012).
[24] B. Podobnik, D. Horvatić, M. Dickison, and H. E. Stanley, Europhys. Lett. **100**, 50004 (2012).
[25] X. Huang, S. Shao, H. Wang, S. V. Buldyrev, H. E. Stanley, and S. Havlin, Europhys. Lett. **101**, 18002 (2013).
[26] G. Dong, L. Tian, R. Du, J. Gao, H. E. Stanley, and S. Havlin, Europhys. Lett. **102**, 68004 (2013).
[27] M. M. Danziger, A. Bashan, Y. Berezin, and S. Havlin, Journal of Complex Networks 2 (4), (2014)
[28] D. Cellai, E. López, J. Zhou, J. P. Gleeson, and G. Bianconi, Phys. Rev. E **88** (5) (2013) 052811.
[29] S. V. Buldyrev, R. Parshani, G. Paul, H. E. Stanley, and S. Havlin, Nature **464**, 1025 (2010).
[30] R. Parshani, S. V. Buldyrev, and S. Havlin, Phys. Rev. Lett. **105**, 048701 (2010).
[31] S. M. Rinaldi, J. P. Peerenboom, and T. K. Kelly, IEEE, 2001
[32] K. Zhao and G. Bianconi, J. Stat. Mech. P05005 (2013).
[33] K. Zhao and G. Bianconi, J. Stat. **152** (2013).
[34] B. Kotnis and J. Kuri, Phys. Rev. E **91**, 032805 (2015).
[35] G. P. Boswell, N. F. Britton and N. R. Franks, Proc. R. Soc. Lond. B **265**, 1921 (1998).
[36] A. Fall, M.-J. Fortin, M. Manseau and D. O'Brien, Ecosys. **10**, 448 (2007).
[37] D. L. Urban, E. S. Minor, E. A. Treml and R. S. Schick, Ecol. Lett. **12**, 260 (2009).
[38] J. M. Tylianakis, E. Laliberté, A. Nielsen and J. Bascompte, Biol. Cons. **143**, 2270 (2010).
[39] G. Huth, A. Lesne, F. Munoz, E. Pitard, Physica A **416**, 290 (2014).
[40] M. E. J. Newman, Phys. Rev. Lett. **89**, 208701 (2002).
[41] S. Maslov and K. Sneppen, Science **296**, 910 (2002).
[42] M. E. J. Newman, Phys. Rev. E **67**, 026126 (2003).
[43] B. Min, S. D. Yi, K.-M. Lee, K.-I. Goh, Phys. Rev. E **89** (2014) 042811.
[44] D. Zhou, H. E. Stanley, G. D'Agostino, and A. Scala, Phys. Rev. E **86**, 066103 (2012).
[45] Pearl, J., *Probabilistic Reasoning in Intelligent Systems: Networks of Plausible Inference* (Morgan Kaufmann, San Francisco, 1988).
[46] Hartmann, A. K., and M. Weigt, *Phase Transitions in Combinatorial Optimization Problems: Basics, Algorithms and Statistical Mechanics* (Wiley-VCH, Berlin, 2005).
[47] M. Mézard and Montanari, *Information, Physics, and Computation* (Oxford University Press, Oxford, 2009).
[48] S. Watanabe and Y. Kabashima, Phys. Rev. E **89**, 012808 (2014).
[49] S. W. Son, G. Bizhani, C. Christensen, P. Grassberger, and M. Paczuski, Europhys. Lett. **97**, 68002 (2012).
[50] M. E. J. Newman, S. H. Strogatz, and D. J. Watts, Phys. Rev. E **64**, 026118 (2001).
[51] The fraction of nodes that are incorrectly evaluated as the constituents of the GC at $t = 3$ in Case F, which are marked with star in Fig. 7, is evaluated 0.02 at most in our study for duplex networks, each layer of which is regular random networks in which degree of node is 4.
[52] J. Hoshen and R. Kopelman, Phys. Rev. B **14**, 3438 (1976).
[53] A. Al-Futaisi and T. W. Patzek, Physica A **321**, 665 (2003).
[54] Y. Watari, S. Nishijima, M. Fukasawa, F. Yamada, S. Abe, and T. Myashita, Ecol. Evol. **3**, 4711 (2013).
[55] K. Fukasawa, T. Miyashita, T. Hashimoto, M. Tatara, and S. Abe, Proc. R. Soc. B: Biol. Sci. **280**, 2075 (2013).